NASA Technical Memorandum 85714

NASA-TM-85714 19840004461

THE DUGDALE MODEL FOR THE COMPACT SPECIMEN

S. Mall and J. C. Newman, Jr.

October 1983

National Aeronautics and Space Administration

Langley Research Center
Hampton, Virginia 23665

THE DUGDALE MODEL FOR THE COMPACT SPECIMEN

S. Mall[1] and J. C. Newman, Jr.[2]
NASA Langley Research Center
Hampton, Virginia 23665

SUMMARY

The purpose of this paper is to develop the Dugdale model for the compact specimen. In particular, plastic-zone size and crack-tip-opening displacement (CTOD) equations were developed. Boundary-collocation analyses were used to analyze the compact specimen subjected to various loading conditions (pin loads, concentrated forces, and uniform pressure acting on the crack surface). Stress-intensity factor and crack-surface displacement equations for some of these loadings were developed and used to obtain the Dugdale model. The results from the equations for plastic-zone size and CTOD agreed well with numerical values calculated by Terada for crack-length-to-width ratios greater than 0.4.

---

[1]Associate Professor, University of Missouri, Rolla, MO 65401.

[2]Senior Scientist, NASA Langley Research Center, Hampton, VA 23665.

NOMENCLATURE

a	crack length measured from centerline of holes
B_j	ratio of b_j to specimen width (b_j/w)
b	distance from crack tip to concentrated force
b_j	dimensions for partially-loaded crack $(j = 1,2)$
c	distance measured from hole centerline to concentrated force
d	crack length plus tensile plastic zone
E	Young's modulus of elasticity
F	boundary-correction factor on stress intensity for pin-loaded hole
G	boundary-correction factor on stress intensity for concentrated force
H	boundary-correction factor on stress intensity for uniform pressure
K	stress-intensity factor
P	pin load per unit thickness on holes
Q	concentrated force per unit thickness on crack surface
r	radius of circular holes
V	crack-surface one-half displacement
w	specimen width
w'	specimen width measured from location of concentrated force
x,y	Cartesian coordinates
z	complex variable, $z = x + iy$
α	crack-length-to-width ratio (a/w)
β	plastic-zone-size-to-width ratio (ρ/w)
γ	equal $\rho/(a + \rho)$
Δ	equal b/w' or $b/(w - a + b)$
η	material constant, $\eta = 0$ for plane stress and $\eta = \nu$ for plane strain
λ	equal $(a + \rho)/w$

ν	Poisson's ratio
ξ	distance measured along crack surface from crack tip
ρ	length of tensile plastic zone
σ	uniform pressure acting on segment of crack surface
σ_0	flow stress of material
Φ, Ψ	complex stress functions

INTRODUCTION

Many aspects of material behavior contribute to the growth of cracks in plates under monotonic and cyclic loading. A general view concerning the behavior of material at the crack tip is that the effects of plastic flow must be accounted for to correlate and to predict the growth of cracks. The Dugdale model [1] is a very simple approach that simulates the effects of plastic flow on plastic-zone size and on crack-tip-opening displacements (CTOD).

The Dugdale model concept has been used with center-crack tension specimens in several fracture analyses [2-4] and in the development of fatigue crack-closure models [5,6] for cracked metallic materials. Currently, the compact specimen is the most widely used specimen for fatigue crack growth rate and fracture toughness testing. The purpose of this paper is to develop the Dugdale model for the compact specimen (Fig. 1(a)). In particular, plastic-zone size (ρ) and CTOD equations have been developed. The Dugdale model is the superposition of two elastic problems. These two elastic problems, a compact specimen subjected to pin loads (P) or to uniform pressure (σ_0) applied to a segment of the crack surfaces, are shown in Fig. 1(b). To develop the Dugdale model for the compact specimen, additional equations for stress-intensity factor (K) and crack-surface displacement (V) must be obtained for this specimen under various loading conditions. These loadings are shown in Fig. 2.

The pin-loaded case, Fig. 2(a), was previously analyzed by Newman [7] to obtain stress-intensity factors and crack-surface displacements. Srawley [8] fitted the results from Ref 7 with a power series to obtain an equation for K. The boundary-collocation method [7] was used herein to analyze a pair of concentrated forces on the crack surfaces (Fig. 2(b)) and a uniform pressure acting on a segment of the crack surfaces (Fig. 2(c)). Both stress-intensity factors and crack-surface displacements under plane-stress conditions (ν = 0.3) were calculated. Stress-intensity factor equations were developed for these loadings. Crack-surface displacement equations were also developed for the pin-loaded case (Fig. 2(a)) and for the uniform-pressure case (Fig. 2(c)) with $b_2 = 0$.

The stress-intensity factor equations for pin loading and uniform pressure ($b_2 = 0$) were used to develop the Dugdale model (plastic-zone size) for the compact specimen. Again, an equation was fitted to these results which gives the plastic-zone size as a function of crack length, specimen width, applied load, and flow stress. Likewise, an equation was developed for the crack-tip-opening displacement (CTOD) for the Dugdale model. The results from these equations were compared with recent numerical results derived by Terada [9].

ANALYSIS OF THE COMPACT SPECIMEN

The boundary-collocation method [7,10] was used to analyze the compact specimen subjected to a pair of concentrated forces, as shown in Fig. 2(b). Some details of the analysis are given in the Appendix. The stress-intensity factors for a wide range of configuration parameters (a/w and b/w') were calculated. The following empirical equation was then fitted to the numerical results

$$K_Q = \frac{2Q}{\sqrt{2\pi b}} G(\alpha,\Delta) \qquad (1)$$

where $\alpha = a/w$ and $\Delta = b/w'$. The correction factor, G, will be presented later.

The crack-surface displacements for the compact specimen subjected to the three types of loading shown in Fig. 2 were calculated by a procedure suggested by Tada, Paris, and Irwin [11]. This procedure is summarized here.

Consider a cracked body loaded by a force system, p, as shown in Fig. 3. Let a pair of virtual forces, q, be applied on the crack surface at the location where the crack-surface displacement is desired. If K_p and K_q are stress-intensity factors due to p and q, respectively, then the crack-surface displacement, V, at location $x = c - d$ is

$$V = \frac{1 - \eta^2}{E} \int_c^d K_p \frac{\partial K_q}{\partial q} da \tag{2}$$

where $\eta = 0$ for plane stress and $\eta = \nu$ for plane strain. For the compact specimen, the partial derivative, $\partial K_q/\partial q$, was obtained from Eq (1) as

$$\frac{\partial K_Q}{\partial Q} = \frac{2G(\alpha,\Delta)}{\sqrt{2\pi b}} = \frac{2G(\alpha,\Delta)}{\sqrt{2\pi(a - c)}} \tag{3}$$

where b is replaced by $(a - c)$ in the function G. During the integration, the crack length c in Eq (2) is held constant (see Fig. 3) while the crack length (a) changes from c to d. The crack length d is the final crack length for which the displacement is desired. Because K_p and K_q are generally complicated functions of crack length, Eq (2) was numerically integrated.

STRESS-INTENSITY FACTORS

Pin-Loaded Holes

As previously mentioned, the standard compact specimen subjected to pin loading, as shown in Fig. 2(a), has been previously analyzed [7]. Stress-intensity factors were calculated for crack-length-to-width ratios ranging from 0.2 to 0.8. Srawley [8] then fitted a polynomial expression to these results and it was

$$K_p = \frac{P}{\sqrt{w}} F\left(\frac{a}{w}\right) \tag{4}$$

where

$$F(\alpha) = (2 + \alpha)\left(0.886 + 4.64\alpha - 13.32\alpha^2 + 14.72\alpha^3 - 5.6\alpha^4\right)/(1 - \alpha)^{3/2} \tag{5}$$

and $\alpha = a/w$. Equation (5) is within ±0.3 percent of the collocation results for $0.2 \leq \alpha < 1$. Equation (4) also approaches the exact asymptotic solution as α approaches unity [12].

Concentrated Forces

The standard compact specimen subjected to a pair of concentrated forces (see Fig. 2(b)) was analyzed by the boundary-collocation method. The stress functions used to exactly satisfy the crack-surface boundary conditions and to approximately satisfy the boundary conditions on the holes and the external boundary are discussed in the Appendix. Stress-intensity factors were calculated for a wide range of configuration parameters. An empirical equation was then fitted to the numerical results and is

$$K_Q = \frac{2Q}{\sqrt{2\pi b}} G\left(\frac{a}{w}, \frac{b}{w}\right) \tag{6}$$

where

$$G(\alpha,\Delta) = \left(1 + A_1\,\Delta + A_2\,\Delta^2\right)\Big/(1 - \Delta)^{3/2} \tag{7}$$

$$A_1 = 3.57 + 12.5(1 - \alpha)^8 \tag{8}$$

$$A_2 = 5.1 - 15.32\alpha + 16.58\alpha^2 - 5.97\alpha^3 \tag{9}$$

$\alpha = a/w$, $\Delta = b/w' = b/(w - a + b)$, and $0 \leq \Delta \leq \alpha$. Equation (6) is within ±0.5 percent of the collocation results for $0.3 \leq \alpha \leq 0.8$ and within ±1 percent for $0.2 \leq \alpha < 0.3$.

Uniform Pressure Acting on a Segment of Crack Surface

With the availability of the K-solution for concentrated forces, the stress-intensity factors for the standard compact specimen subjected to a uniform pressure, σ, acting on a segment (b_1 to b_2) of the crack surface, shown in Fig. 2(c), can be determined using the Green's function concept. The stress-intensity factor is then given by

$$K_\sigma = \int_{b_2}^{b_1} \frac{2\sigma}{\sqrt{2\pi b}}\,G\,db \tag{10}$$

Integration of Eq (10) for uniform pressure gives

$$K_\sigma = \sigma\sqrt{\frac{w}{8\pi}}\,H\left(\frac{a}{w},\frac{b_1}{w},\frac{b_2}{w}\right) \tag{11}$$

$$H = \frac{1}{(1 - \alpha)^{3/2}}\Big[2B\left(1 + A_1 + A_2\right)\sqrt{B^2 + (1 - \alpha)B}$$

$$+ (1 - \alpha)\left(5 + A_1 - 3A_2\right)\sqrt{B^2 + (1 - \alpha)B}$$

$$+ (1 - \alpha)^2\left(3 - A_1 + 3A_2\right)\ln\left(\sqrt{B} + \sqrt{B + 1 - \alpha}\right)\Big]\Big|_{B = B_2}^{B = B_1} \tag{12}$$

where $\alpha = a/w$ and $B_j = b_j/w$. The functions A_1 and A_2 are given by Eqs (8) and (9), respectively. Because the concentrated force solution was within ±0.5 percent of the collocation results, the uniform pressure case would have the same accuracy for $0 \leq B_j \leq \alpha$ and $0.3 \leq \alpha \leq 0.8$. Equation (11) is useful in developing the Dugdale model and plastic-zone size equations for the compact specimen. This development will be discussed later.

CRACK-SURFACE DISPLACEMENTS

Pin-Loaded Holes

The crack-surface displacements for the compact specimen under pin loading (Fig. 2(a)) for plane-stress conditions were previously calculated using a collocation analysis [7,13]. For comparison, the displacements were also calculated from Eq (2). The crack-surface displacement, V_p, under plane-stress conditions at a distance c from the hole centerline is

$$V_p = \frac{2P}{E} \int_{c/w}^{\alpha} \frac{F(\alpha)G(\alpha,\Delta)}{\sqrt{2\pi(\alpha - c/w)}}\, d\alpha \qquad (13)$$

Equation (13) was numerically integrated. Because the polynomial expressions for F and G (Eqs (5) and (7), respectively) are within ±0.5 percent of the collocation results for $0.3 \leq \alpha \leq 0.8$, then the computation of crack-surface displacement would, in general, be within ±1 percent of the collocation results. The normalized displacements, EV_p/P, as functions of ξ/a, are shown in Fig. 4 for various values of a/w. The symbols show calculations from Eq (13) and the curves were obtained from a boundary-collocation analysis [13]. The results from numerical integration and collocation agreed within 1 percent. Equation (13) cannot be used for locations $\xi/a > 1 - 0.2(w/a)$ because F and G were not developed for a/w ratios less than 0.2.

For ease of computation, a polynomial expression for the normalized displacements shown in Fig. 4 was developed. This expression is

$$\frac{EV_p}{P} = 4\sqrt{\frac{\xi}{2\pi w}}\left[1 + C_1\left(\frac{\xi}{a}\right) + C_2\left(\frac{\xi}{a}\right)^2\right]F \tag{14}$$

$$C_1 = -1.25 + 9.76\alpha - 20.15\alpha^2 + 16.62\alpha^3$$

$$C_2 = 0.64 - 4.34\alpha + 10.24\alpha^2 - 8.46\alpha^3$$

where $\alpha = a/w$ and F is given by Eq (5). Equation (14) is within ±1 percent of the numerical results from Eq (13) for $\xi/a < 1 - 0.2/\alpha$ and $0.3 \leq \alpha \leq 0.8$.

Concentrated Forces

The crack-surface displacements for the compact specimen subjected to a pair of concentrated forces (Q) (Fig. 2(b)) under plane-stress conditions were calculated using either the collocation analysis (see Appendix) or Eq (2). Using Eq (2), the crack-surface displacement, V_Q, at a distance c from the hole centerline is

$$V_Q = \frac{2Q}{\pi E}\int_{c/w}^{\alpha} \frac{G(\alpha,\Delta_0)G(\alpha,\Delta)}{\sqrt{(\alpha - c/w)b_0/w}}\,d\alpha \tag{15}$$

where $\Delta_0 = b_0/(w - a + b_0)$ in Eq (7). The distance b_0 is the location of the stationary force Q. The distance b is the location of the virtual force q. Again, b must be replaced by $(a - c)$ and b_0 must be replaced by $(a - c_0)$. The distance c_0 is the distance from the hole centerline to the location of the force Q. Again, Eq (15) was numerically integrated.

The normalized displacements, EV_Q/Q, as functions of ξ/a, are shown in Fig. 5 for various values of a/w. The symbols show calculations from Eq (15),

and the curves were obtained from the boundary-collocation analysis. The results from numerical integration and collocation again agreed well. Again, Eq (15) cannot be used for locations $\xi/a > 1 - 0.2(w/a)$ because G was not developed for a/w ratios less than 0.2.

Uniform Pressure Acting on a Segment of Crack Surface

The crack-surface displacements for the compact specimen subjected to a uniform pressure, as shown in Fig. 2(c), were also calculated using Eq (2). The displacement, V_σ, at a distance c from the hole centerline is

$$V_\sigma = \frac{\sigma w}{2\pi E} \int_{c/w}^{\alpha} \frac{H(\alpha, B_1, B_2) G(\alpha, \Delta)}{\sqrt{\alpha - c/w}} \, d\alpha \tag{16}$$

where G and H are given by Eqs (7) and (12), respectively. The function B_j is b_j/w, and b_j must be replaced by $(a - c_j)$. The distance c_j is measured from the hole centerline to appropriate ends of the uniform pressure loading.

Some typical normalized crack-surface displacements, $EV_\sigma/(\sigma w)$, with $a/w = 0.6$ for various lengths of uniform pressure are shown in Fig. 6. The displacements calculated from Eq (16), shown as symbols, were within 1 percent of displacements calculated from collocation (curves) because the polynomial expressions for G and H (Eqs (7) and (12), respectively) are within ±0.5 percent of collocation results. These displacements are useful in developing the CTOD equations for the Dugdale model.

DUGDALE MODEL FOR COMPACT SPECIMEN

The Dugdale model for the compact specimen (Fig. 1) requires that the "finiteness" condition of Dugdale be satisfied. This condition states that the

K at the tip of the plastic zone (at $d = a + \rho$) is zero. From this condition, the plastic-zone size (ρ) was calculated for various a/w and $P/(w\sigma_o)$ ratios. An equation was then fitted to these results and was

$$\frac{\rho}{a} = \frac{\pi w}{8a}\left(\frac{PF}{w\sigma_o}\right)^2 F_o \tag{17}$$

where

$$F = (2 + \alpha)\left(0.886 + 4.64\alpha - 13.32\alpha^2 + 14.72\alpha^3 - 5.6\alpha^4\right)/(1 - \alpha)^{3/2}$$

$$F_o = 1 + f_1\left(\frac{P}{w\sigma_o}\right) + f_2\left(\frac{P}{w\sigma_o}\right)^2$$

$$f_1 = -2.687(1 - \alpha) + 0.167/\alpha^2$$

$$f_2 = -2.48 - 0.039/(1 - \alpha)^6$$

and $\alpha = a/w$. Equation (17) is within ±1 percent of the current collocation results for $0.3 \leq (a + \rho)/w \leq 0.8$ and $\rho/(w - a) \leq 0.5$. A comparison of plastic-zone sizes calculated from Eq (17) and some recent collocation results from Terada [9] are shown in Fig. 7. The normalized plastic-zone size, $\rho/(w - a)$, is plotted against $P/(w\sigma_o)$ for various values of a/w. The curves show the present results (Eq (17)) and they agreed well with the previous results from Terada (symbols).

In the compact specimen, the material at point A in Fig. 1(a) is in compression. At a certain load, this material will yield in compression. From a finite-element-strip-yield analysis for an elastic-perfectly plastic material,

the load that causes incipient yielding at point A was calculated. For each value of a/w, these loads are shown as the upper ends of the solid curves. The upper ends of the dashed curves denote loads and plastic-zone sizes where backface yielding at point A has about a 2 percent effect on crack-tip-opening displacement (CTOD). Thus, Eq (17) is restricted to

$$\frac{\rho}{w - a} \leq 0.53 - 0.65\alpha + 0.32\alpha^2 \tag{18}$$

so that the influence of backface yielding on CTOD is less than 2 percent. The influence of backface yielding on plastic-zone size is not included in Eq (17).

The CTOD ($2V_a$) for the compact specimen was calculated by adding the displacement at the tip of the physical crack length (a) due to the pin load and due to the uniform stress. Again, an equation was fitted to these results and was

$$\frac{2V_a E}{P} = 8\sqrt{\frac{\beta}{2\pi}}\, F_1 F_2 - \frac{w\sigma_o}{\pi P}\sqrt{\beta}\, H_1 H_2 \tag{19}$$

where

$$F_1 = (2 + \lambda)\left(0.886 + 4.64\lambda - 13.32\lambda^2 + 14.72\lambda^3 - 5.6\lambda^4\right)/(1 - \lambda)^{3/2}$$

$$F_2 = 1 + B_1\gamma + B_2\gamma^2$$

$$B_1 = -1.25 + 9.76\lambda - 20.15\lambda^2 + 16.62\lambda^3$$

$$B_2 = 0.64 - 4.34\lambda + 10.24\lambda^2 - 8.46\lambda^3$$

$$H_1 = \left\{\left[2\beta\left(1 + A_1 + A_2\right) + (1 - \lambda)\left(5 + A_1 - 3A_2\right)\right]\sqrt{\beta^2 + (1 - \lambda)\beta} + (1 - \lambda)^2\left(3 - A_1 + 3A_2\right)\left[\ln\left(\sqrt{\beta} + \sqrt{\beta + 1 - \lambda}\right) - \ln\sqrt{1 - \lambda}\right]\right\}/(1 - \lambda)^{3/2}$$

$$A_1 = 3.57 + 12.5(1 - \lambda)^8$$

$$A_2 = 5.1 - 15.32\lambda + 16.58\lambda^2 - 5.97\lambda^3$$

$$H_2 = 1 + h_1\gamma + h_2\gamma^2$$

$$h_1 = 0.666 + 0.796\lambda^2 + 12.36\lambda^4$$

$$h_2 = 0.084 + 2.62\lambda^2 - 14.08\lambda^4$$

$\beta = \rho/w$, $\lambda = (a + \rho)/w$, and $\gamma = \rho/(a + \rho)$.

Equation (19) is within about ±1.5 percent of the current collocation results for $0.3 \leq \lambda \leq 0.8$, $\gamma \leq 1 - 0.2/\lambda$, and $\rho/(w - a) \leq 0.5$. Figure 8 shows the normalized displacement against plastic-zone-size-to-ligament ratio for various a/w ratios. The curves show the results from Eq (19) and the symbols show results from Terada [9]. The results agreed well. The slight discrepancy at an a/w ratio of 0.3 was probably due to neglecting the pin-loaded holes in Terada's analysis. Again the dashed curves indicate that back-face yielding is occurring, but its influence on CTOD is less than 2 percent if the plastic-zone size is less than that given by Eq (18).

CONCLUDING REMARKS

A two-dimensional elastic boundary-collocation analysis was used to analyze the compact specimen subjected to various loading conditions. The effects of the pin holes were included. The loading cases were: pin-loaded holes, a pair of concentrated forces acting on the crack surfaces, and a uniform pressure acting over a segment of the crack surfaces. Stress-intensity factor (K) equations were developed for each of these loadings. Crack-surface displacement (V) equations were also developed for pin-loaded holes and for some

restricted configurations of the uniform pressure case. The K-equations were within ±0.5 percent and the V-equations were within ±1 percent of the collocation results. Some of these equations were used to develop algebraic equations for plastic-zone size and crack-tip-opening displacement (CTOD) for the Dugdale model. The plastic-zone size and CTOD equations were within 1 and 1.5 percent, respectively, of the collocation results.

The results from this study on the compact specimen can be used in various analyses based on the Dugdale model concept. Some examples are the critical CTOD fracture analyses and the crack-closure models.

APPENDIX

STRESS-INTENSITY FACTOR EQUATION FOR CONCENTRATED FORCES APPLIED TO CRACK SURFACES ON COMPACT SPECIMENS

The stress-intensity factors for a compact specimen subjected to a pair of concentrated forces on the crack surfaces, Fig. 2(b), were obtained from a boundary-collocation analysis. An algebraic equation was fitted to the numerical stress-intensity factors.

For the compact specimen configuration, consider a semi-infinite crack along the x-axis in an infinite plate subjected to a pair of concentrated forces, Q, as shown in Fig. 9. The dashed lines L_1 and L_2 define the boundaries of the compact specimen. The Muskhelishvili [14] stress functions for this configuration are

$$\left.\begin{aligned} \Phi(z) &= \Phi_0(z) + \Phi_1(z) + \Phi_2(z) \\ \Psi(z) &= \Psi_0(z) + \Psi_1(z) + \Psi_2(z) \end{aligned}\right\} \tag{20}$$

The subscripts denote functions which are needed to satisfy conditions for the concentrated forces on the crack surfaces and to approximately satisfy conditions on boundaries L_1 and L_2, respectively.

The stress functions for a semi-infinite crack in an infinite plate subjected to a pair of concentrated forces on the crack surface were derived from equations given in Ref 15. They are

$$\Phi_0(z) = \Psi_0(z) = \frac{Q}{\pi} \tan^{-1} \sqrt{\frac{z}{b}} \tag{21}$$

The stress functions used to approximately satisfy boundary conditions on the external boundary L_1 are

$$\left.\begin{matrix}\Phi_1(z)\\ \Psi_1(z)\end{matrix}\right\} = \sqrt{z}\sum_{n=1}^{N} A_n z^{n-1} \pm \sum_{n=1}^{N} B_n z^n \tag{22}$$

where the coefficients A_n and B_n are real. The stress functions will, of course, produce stresses on the internal boundary L_2.

The stress functions used to approximately satisfy boundary conditions on boundary L_2 are

$$\begin{aligned}\left.\begin{matrix}\Phi_2(z)\\ \Psi_2(z)\end{matrix}\right\} &= \sqrt{z}\sum_{n=1}^{M} C_n i\left[(z - z_h)^{-n} - (z - \bar{z}_h)^{-n}\right]\\ &+ \sqrt{z}\sum_{n=1}^{M} D_n\left[(z - z_h)^{-n} + (z - \bar{z}_h)^{-n}\right]\\ &\pm \sum_{n=1}^{M} \tilde{C}_n i\left[((z - z_h)^{-n} - (z - \bar{z}_h)^{-n}\right]\\ &\pm \sum_{n=1}^{M} \tilde{D}_n\left[(z - z_h)^{-n} + (z - \bar{z}_h)^{-n}\right]\end{aligned} \tag{23}$$

where C_n, $\tilde{C}_n$, D_n, and $\tilde{D}_n$ are real. In these stress functions, poles z_h and $\bar{z}_h$ were located at the centers of the two holes (see Fig. 9). The stress functions in Eqs (22) and (23) automatically satisfy the conditions of stress-free crack surfaces and the single-valuedness of displacement condition for multiply connected regions. The conditions on boundaries L_1 and L_2 were approximately satisfied by the series solution using the boundary-collocation method described in Ref 10. From a convergence study, N was selected as 40 and M was 20.

The stress-intensity factor is given by

$$K = 2\sqrt{2\pi}\lim_{z\to 0}\sqrt{z}\,\Phi'(z) \tag{24}$$

They were calculated for a wide range in configuration parameters. An empirical equation was fitted to the numerical stress-intensity factors and is

$$K = \frac{2Q}{\sqrt{2\pi b}} G\left(\frac{a}{w}, \frac{b}{w'}\right) \tag{25}$$

The equation for the correction factor, G, is

$$G(\alpha,\Delta) = \left(1 + A_1\Delta + A_2\Delta^2\right)\Big/(1 - \Delta)^{3/2} \tag{26}$$

$$A_1 = 3.57 + 12.5(1 - \alpha)^8$$

$$A_2 = 5.1 - 15.32\alpha + 16.58\alpha^2 - 5.97\alpha^3$$

where $\alpha = a/w$, $\Delta = b/w'$, $0 \leq \Delta \leq \alpha$, and $0.2 \leq \alpha \leq 0.8$. Equation (25) is within ±0.5 percent of the boundary-collocation results for $0.3 \leq \alpha \leq 0.8$ and within ±1 percent for $0.2 \leq \alpha < 0.3$. For clarity, only the results for a/w ratios of 0.3, 0.5, and 0.8 are shown in Fig. 10. The curves were calculated from Eq (26).

REFERENCES

[1] Dugdale, D. S., Yielding of Steel Sheets Containing Slits, Journal of the Mechanics and Physics of Solids, vol. 8, 1960, pp. 100-104.

[2] Newman, J. C., Jr., "Fracture of Cracked Plates Under Plane Stress," Engineering Fracture Mechanics, vol. 1, no. 1, 1968, pp. 137-154.

[3] Heald, P. T., Spinks, G. M., and Worthington, P. J., "Post-Yield Fracture Mechanics," Material Science and Engineering, vol. 10, 1972, pp. 129-138.

[4] Larsson, L. H., "Use of EPFM in Design," Advances in Elasto-Plastic Fracture Mechanics, Applied Science Publishers, Ltd., Essex, England, 1979, pp. 261-278.

[5] Dill, H. D. and Saff, C. R., "Spectrum Crack Growth Prediction Method Based on Crack Surface Displacement and Contact Analyses," Fatigue Crack Growth Under Spectrum Loads, ASTM STP 595, American Society for Testing and Materials, 1976, pp. 306-319.

[6] Newman, J. C., Jr., "A Crack-Closure Model for Predicting Fatigue-Crack Growth Under Aircraft Spectrum Loading," Methods and Models for Predicting Fatigue Crack Growth Under Random Loading, ASTM STP 748, American Society for Testing and Materials, 1981, pp. 53-84.

[7] Newman, J. C., Jr., "Stress Analysis of Compact Specimens Including the Effects of Pin Loading," Fracture Analysis, ASTM STP 560, American Society for Testing and Materials, 1974, pp. 105-121.

[8] Srawley, J. E., "Wide Range Stress-Intensity Factor Expressions for ASTM E399 Standard Fracture Toughness Specimens, International Journal of Fracture Mechanics, vol. 12, 1976, pp. 475-476.

[9] Terada, H., "Elastic and Elasto-Plastic Stress Analysis of the Standard Compact Tension Specimen," Journal of Pressure Vessel Technology, vol. 105, 1983, pp. 132-137.

[10] Newman, J. C., Jr., "Stress Analysis of Simply and Multiply Connected Regions Containing Cracks by the Method of Boundary Collocation," M.S. Thesis, Virginia Polytechnic Institute, Blacksburg, VA, May 1969.

[11] Tada, H., Paris, P. C., and Irwin, G. R., The Stress Analysis of Cracks Handbook, Del Research Corporation, Hellertown, PA, 1973.

[12] Bentham, J. T. and Koiter, W. T., "Asymptotic Approximations to Crack Problems," Mechanics of Fracture I--Methods of Analysis and Solution of Crack Problems, Noordhoff International Publications, 1973, pp. 159-162.

[13] Newman, J. C., Jr., "Crack-Opening Displacements in Center-Crack, Compact, and Crack-Line-Wedge-Loaded Specimens," NASA TN D-8268, National Aeronautics and Space Administration, July 1976.

[14] Muskhelishvili, N. I., Some Basic Problems of Mathematical Theory of Elasticity, P. Noordhoff, 1953.

[15] Erdogan, F., "On the Stress Distribution in Plates with Collinear Cuts under Arbitrary Loads," Proceedings of Fourth U.S. National Congress of Applied Mechanics, vol. 1, American Society of Mechanical Engineers, 1962, pp. 547-553.

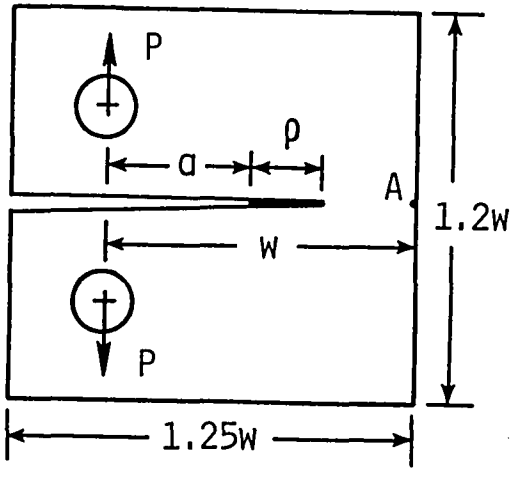

(a) "Dugdale" yield model.

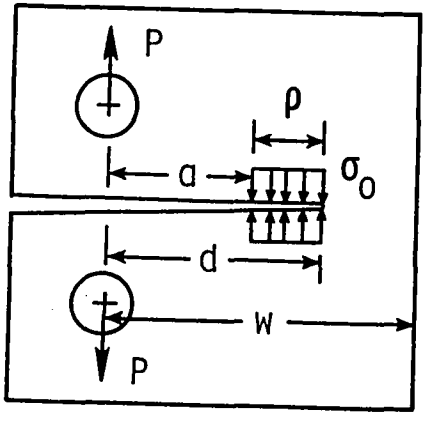

(b) Equivalent elastic loading.

Fig. 1--Dugdale model for the compact specimen.

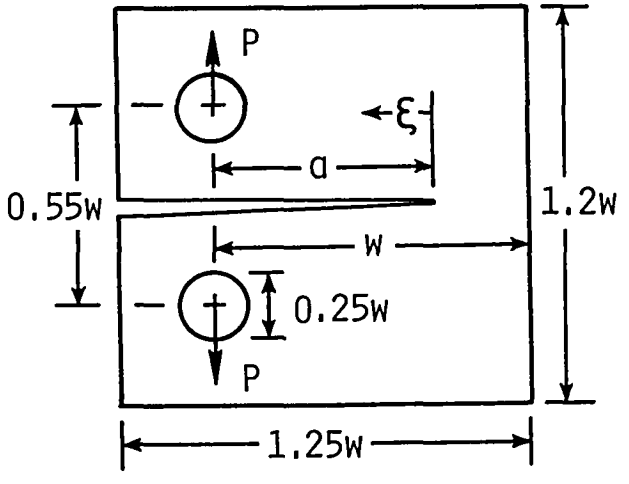

(a) Pin-loaded holes.

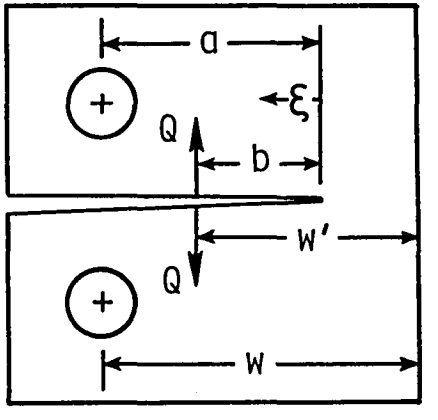

(b) Concentrated forces.

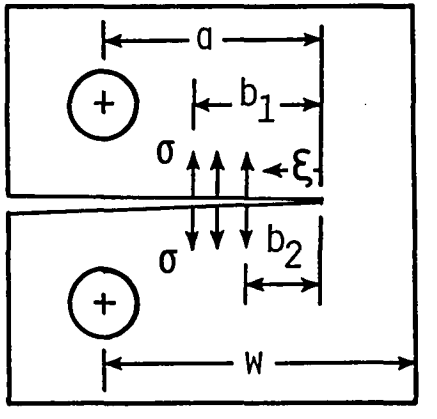

(c) Uniform pressure.

Fig. 2--Compact specimen configuration subjected to various loading.

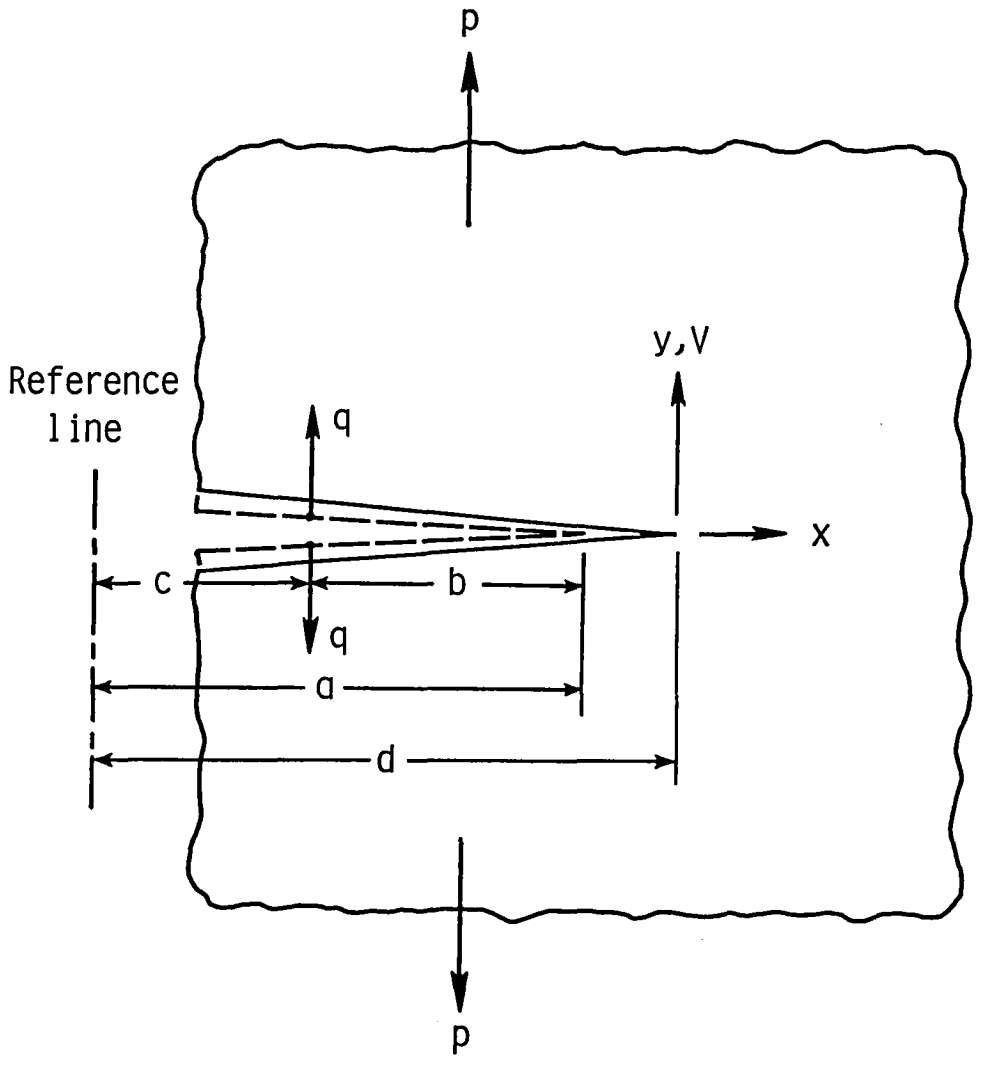

Fig. 3--Crack in arbitrary-shaped plate (symmetric about x-axis) subjected to an applied force system, p, and virtual forces, q.

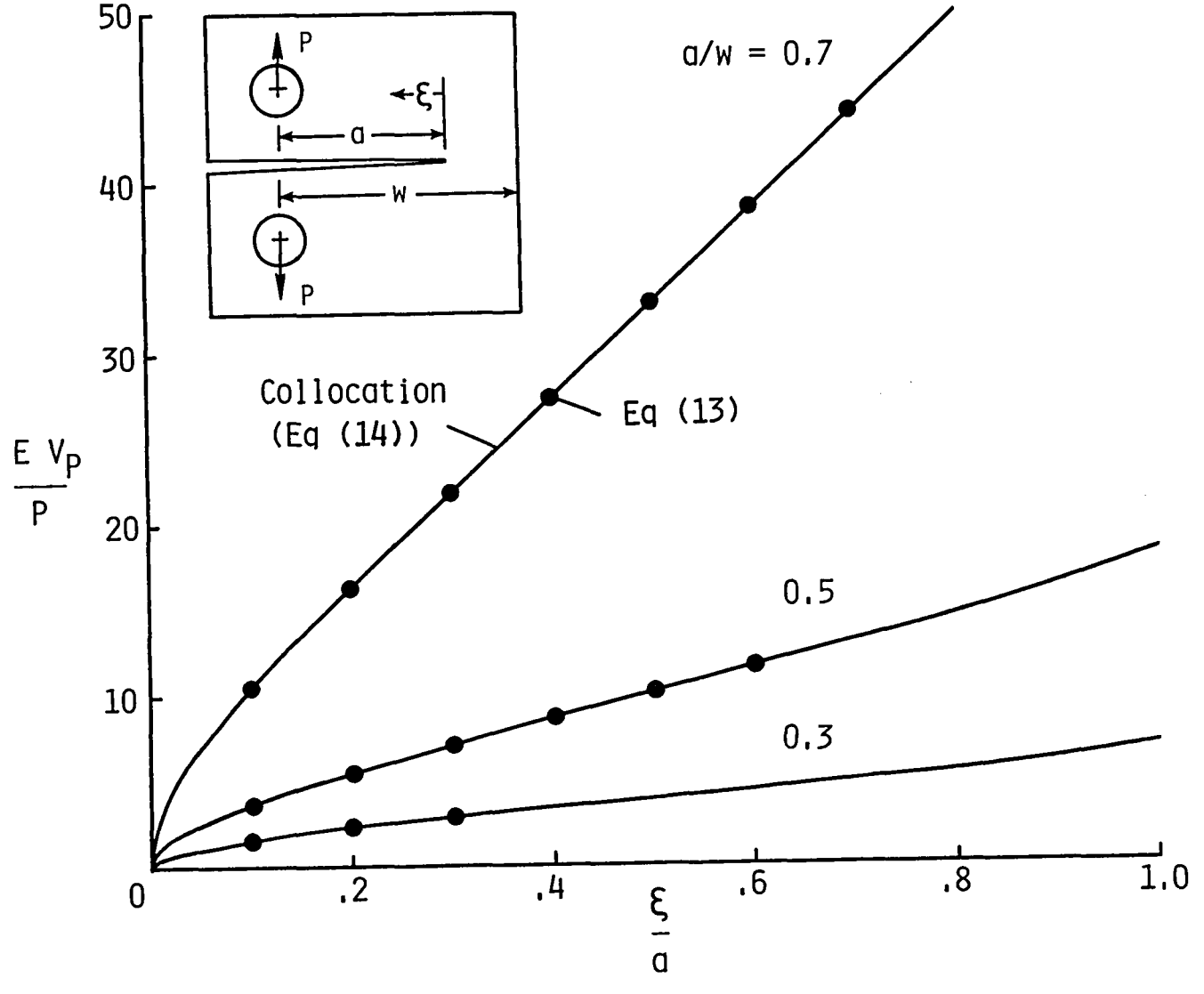

Fig. 4--Normalized crack-surface displacement for compact specimen with pin-loaded holes for various a/w ratios.

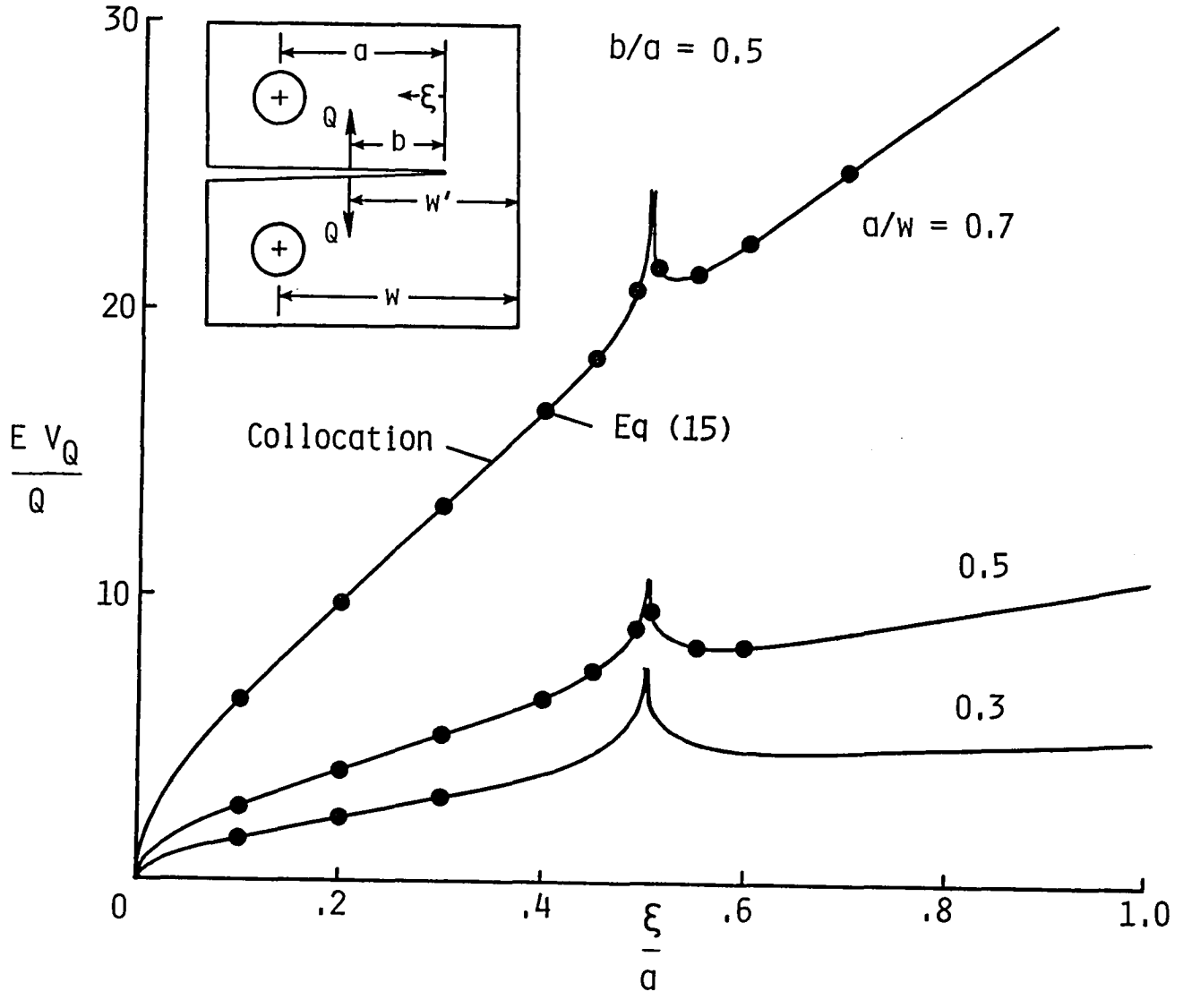

Fig. 5--Normalized crack-surface displacement for compact specimen with concentrated forces on crack surface at b/a = 0.5 for various a/w ratios.

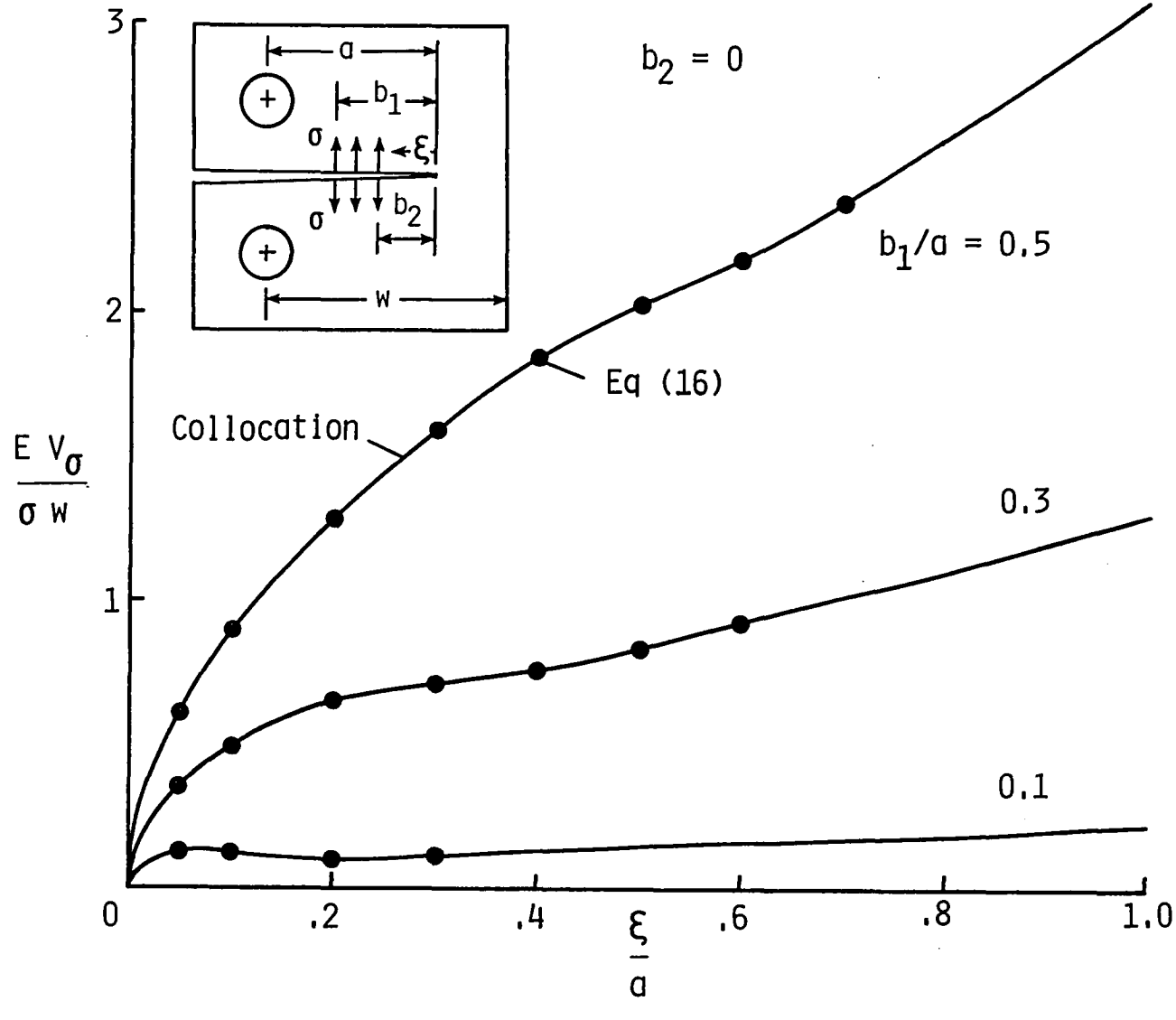

Fig. 6--Normalized crack-surface displacement for compact specimen with uniform pressure applied to crack surface ($b_2 = 0$) for various b_1/a ratios.

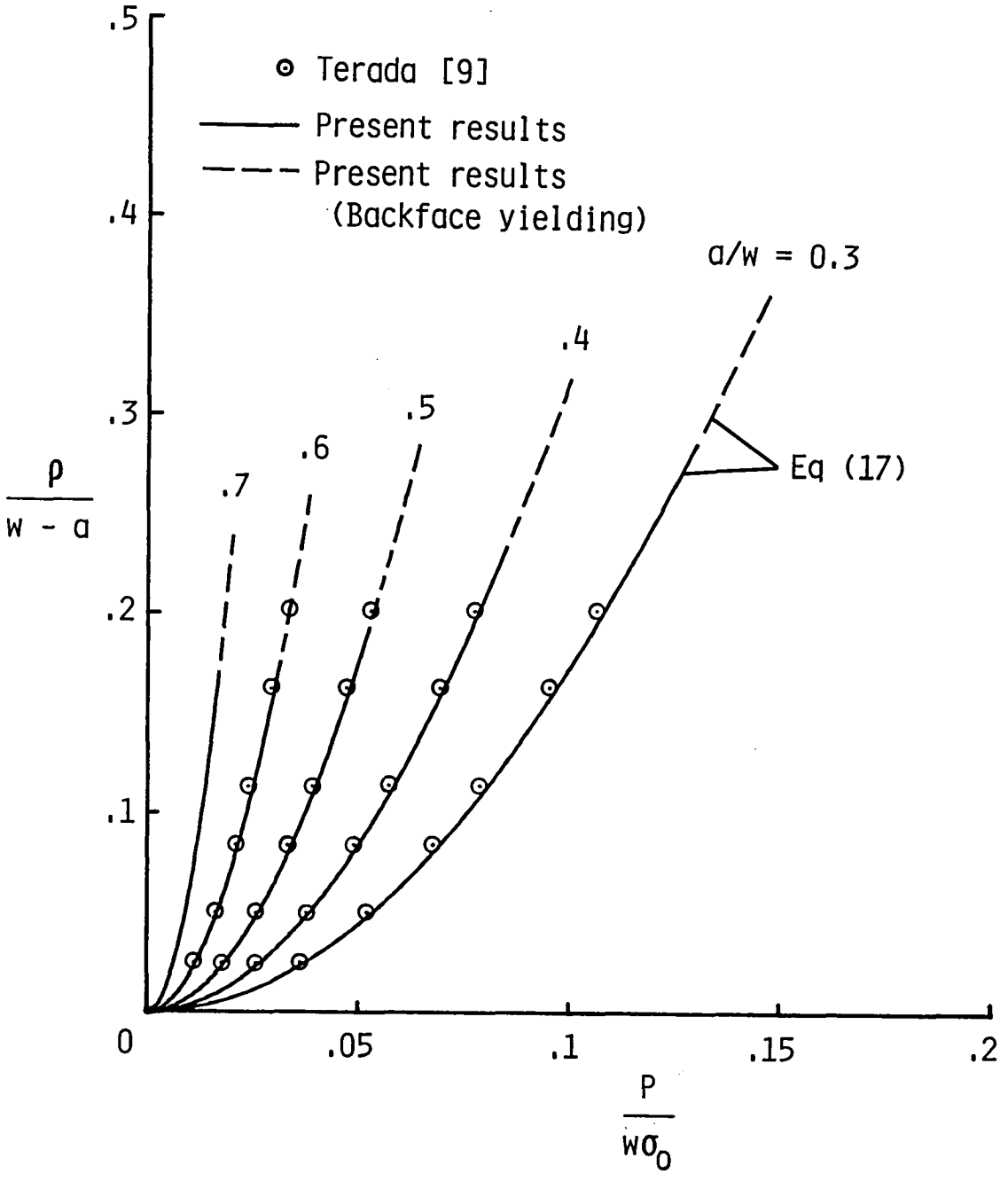

Fig. 7--Comparison of normalized plastic-zone size against applied load for various a/w ratios.

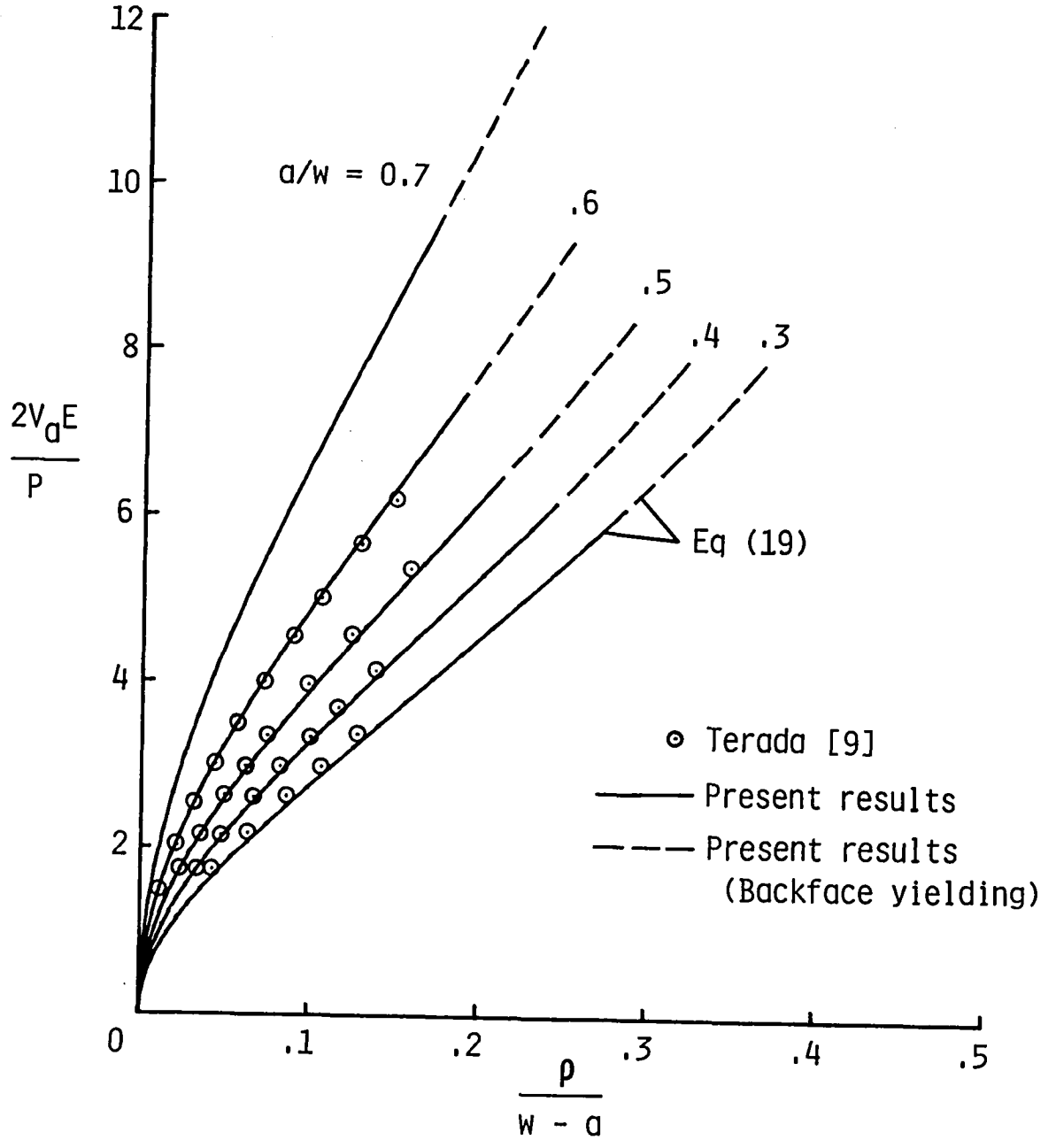

Fig. 8--Comparison of crack-tip-opening displacement against plastic-zone size for various a/W ratios.

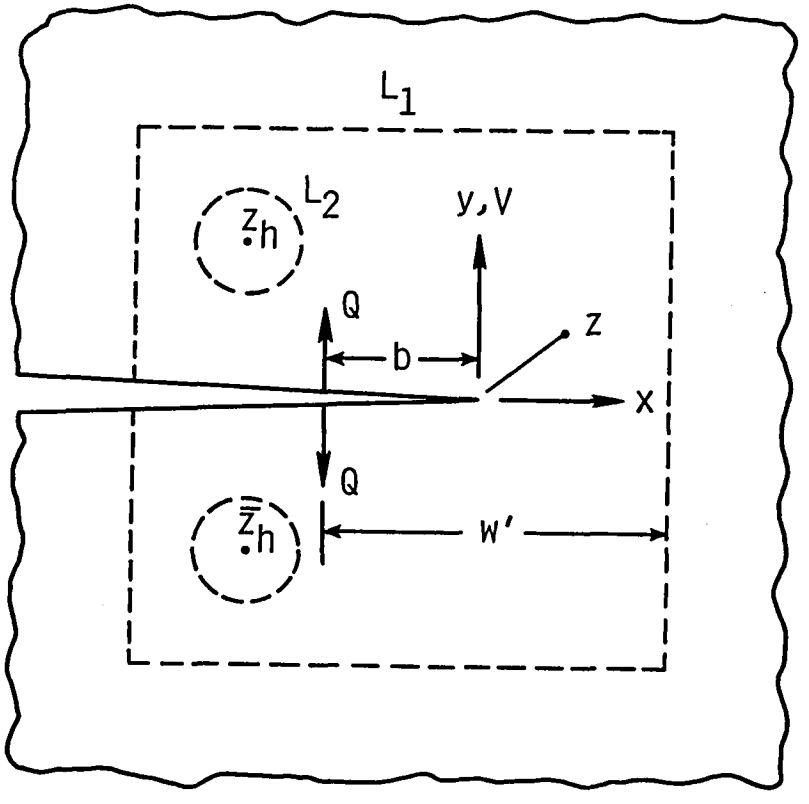

Fig. 9--Crack in infinite plate subjected to pair of concentrated forces on crack surface.

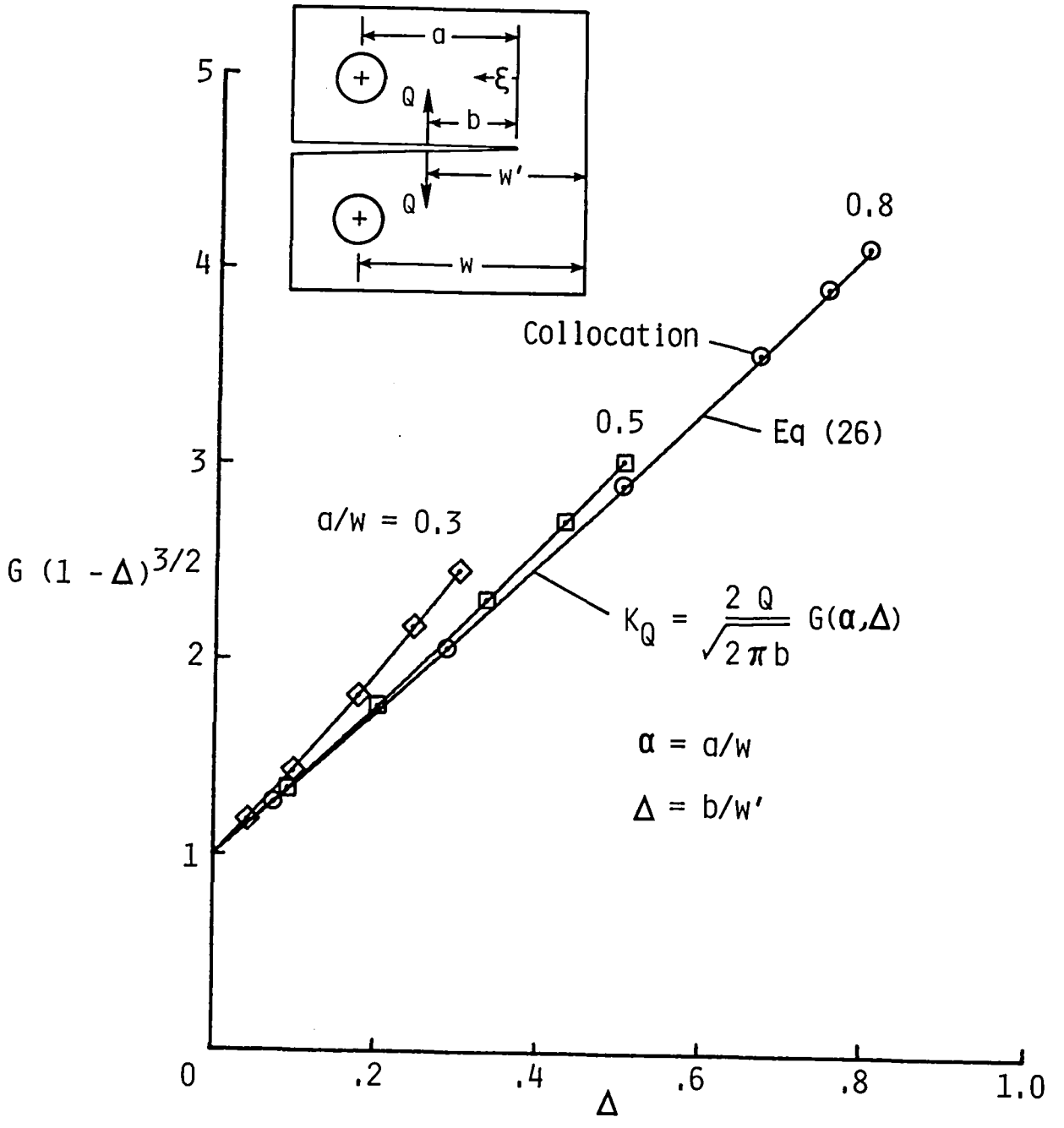

Fig. 10--Boundary-correction factors for compact specimen with pair of concentrated forces, Q, applied to crack surface.

1. Report No.	2. Government Accession No.	3. Recipient's Catalog No.
NASA TM-85714		

4. Title and Subtitle	5. Report Date
THE DUGDALE MODEL FOR THE COMPACT SPECIMEN	October 1983
	6. Performing Organization Code 505-33-23-02

7. Author(s)	8. Performing Organization Report No.
S. Mall* and J. C. Newman, Jr.	
	10. Work Unit No.

9. Performing Organization Name and Address	11. Contract or Grant No.
NASA Langley Research Center Hampton, VA 23665	
	13. Type of Report and Period Covered Technical Memorandum

12. Sponsoring Agency Name and Address	14. Sponsoring Agency Code
National Aeronautics and Space Administration Washington, DC 20546	

15. Supplementary Notes *University of Missouri, Rolla, Missouri.

Presented at the ASTM 16th National Symposium on Fracture Mechanics, Columbus, Ohio, August 15-18, 1983.

16. Abstract

The purpose of this paper is to develop the Dugdale model for the compact specimen. In particular, plastic-zone size and crack-tip-opening displacement (CTOD) equations were developed. Boundary-collocation analyses were used to analyze the compact specimen subjected to various loading conditions (pin loads, concentrated forces, and uniform pressure acting on the crack surface). Stress-intensity factor and crack-surface displacement equations for some of these loadings were developed and used to obtain the Dugdale model. The results from the equations for plastic-zone size and CTOD agreed well with numerical values calculated by Terada for crack-length-to-width ratios greater than 0.4.

17. Key Words (Suggested by Author(s))		18. Distribution Statement
Compact specimen	Displacements	Unclassified - Unlimited
Plastic deformation	Cracks	
Stress functions	Collocation	Subject Category 39
Fracture strength		
Crack propagation		

19. Security Classif. (of this report)	20. Security Classif. (of this page)	21. No. of Pages	22. Price*
Unclassified	Unclassified	30	A03

* For sale by the National Technical Information Service, Springfield, Virginia 22161